Soft mode dynamics and the reduction of Ti^{4+} disorder in ferroelectric/relaxor superlattices $BaTiO_3/BaTi_{0.68}Zr_{0.32}O_3$

F. De Guerville, M. El Marssi,* I. P. Raevski,† M. G. Karkut, and Yu. I. Yuzyuk†
Laboratoire de Physique de la Matière Condensée, Université de Picardie Jules Verne, 33 rue Saint-Leu, 80039 Amiens Cedex, France
(Received 11 May 2006; revised manuscript received 7 July 2006; published 10 August 2006)

We used pulsed laser deposition to grow a series of $[BaTiO_3]_{\Lambda/2}/[BaTi_{0.68}Zr_{0.32}O_3]_{\Lambda/2}$ (BTZ/BT) superlattices (SL's) with a modulation period Λ that varies between 16 Å$\leqslant\Lambda\leqslant$1008 Å; the total thickness is kept constant at about 4000 Å. We determine the out-of-plane lattice parameters of the SL constituents by modeling the x-ray diffractograms of the SL's. The results indicate that the polar *c* axis of the BT layers lies in the plane of the film. The Raman data reinforces this interpretation. The Raman spectra of SL's give evidence of coupling between BT and BTZ layers and a narrowing of the Raman peaks suggest a reduction of the disorder of the Ti^{4+} ions due to the strain. This strain resulting from the lattice mismatch between the constituent layers is responsible for the upward frequency shift of the soft modes, especially the E(1TO) mode, which is markedly altered with respect to its analogs in BT-bulk crystals and BT film. This soft-mode behavior as a function of Λ indicates that the crystal structure of all SL's is more rigid than in BTZ and BT single thin films.

DOI: 10.1103/PhysRevB.74.064107 PACS number(s): 77.84.−s, 68.65.Cd, 78.30.−j

Ferroelectric superlattices (SL's) constructed by alternating coherent layers of different perovskites have attracted much interest in recent years due to the possibility of producing superior properties that are attractive for thin-film device applications. Physical properties different from those of ordinary ferroelectric films can be obtained in the SL structure by modifying of the lattice by strain within the constituent layers.[1–11] $BaTiO_3$ (BT), because it has been so extensively studied in bulk and thin film form, is often a material of choice in the construction of ferroelectric SL's. Enhancement of the dielectric properties[1] and the remanent polarization[4] were observed in ferroelectric/paraelectric $BaTiO_3/SrTiO_3$ (BT/ST) SL's. Recently, Das *et al.*[12] reported significant soft-mode hardening and activation of folded acoustical modes in BT/ST SL's. Le Marrec *et al.*[13] constructed ferroelectric/ferroelectric SL's consisting of layers of BT and $PbTiO_3$ (PT) and they demonstrated the existence of confined vibrational modes in short wavelength BT/PT SL's. To the best of our knowledge there have been no published studies on BT/relaxor SL's, even though relaxor ferroelectrics can have excellent dielectric and electromechanical properties.[14,15] The potential impact of SL's composed of relaxors is stimulated by strain effects, which can dramatically modify their physical properties.[16,17] Very recently we have reported[18] the first work on ferroelectric/relaxor SL's consisting of alternating layers PT and $PbMg_{1/3}Nb_{2/3}O_3$ (PMN) for which a significant change in the vibrational behavior of the constituents was observed.

Nominally cubic at all temperatures, relaxors are characterized by a strong frequency dependence of the broad permittivity peak as a function of temperature, which distinguishes them from classic ferroelectrics, such as BT, which exhibit well-defined phase transitions with a sharp peak in the permittivity. For doped BT, a crossover from ferroelectic to relaxor behavior is observed beyond a certain doping level. Zirconium modified solid solutions $BaTi_{1-x}Zr_xO_3$ (BTZ) are ferroelectrics up to $x=0.27$, and beyond this value they exhibit relaxorlike properties.[19,20] Hence due to their fundamental interest as well as to environmental concerns, several studies have been devoted to these lead-free relaxors over the last few years.[19–21]

Here we report the fabrication, structural and Raman scattering characterization of lead-free ferroelectric/relaxor SL's as a function of modulation wavelength Λ. In proper ferroelectrics the polar soft mode is the primary order parameter and it is very sensitive to the strain effects in single thin films and SL's. The aim of this work is the study of soft-mode behavior in artificial SL's where ferroelectric BT layers alternate with BTZ relaxor layers. The BT (bulk lattice parameters: $a_{BT}=3.992$ Å, $c_{BT}=4.036$ Å) and the relaxor BTZ with $x=0.32$ (bulk $a_{BTZ}=4.055$ Å) were grown on cubic single-crystal (001) MgO substrates ($a_{MgO}=4.213$ Å) buffered with a 50 Å-thick oxide layer of $La_{1/2}Sr_{1/2}CoO_3$ (LSCO, $a_{LSCO}=3.805$ Å). We grew seven SL's of $BT_{\Lambda/2}/BTZ_{\Lambda/2}$ with modulation periods $\Lambda=16$, 32, 64, 126, 252, 504, and 1008 Å. The total thickness of each SL was approximately 4032 Å.

The samples were grown by pulsed laser deposition (PLD) using a Lambda Physik 248 nm excimer laser in a MECA 2000 UHV chamber. An epitaxial LSCO buffer layer was deposited at a substrate temperature of 700 °C in an oxygen partial pressure of 0.2 mbar. The temperature and oxygen pressure during BT and BTZ layers deposition were 750 °C and 0.1 mbar, respectively. A deposition rate of 0.26 Å/pulse was determined from x-ray thickness (Laue) oscillations observed on very thin films of BT and of BTZ. The surface quality of the layers was monitored using reflection high-energy electron diffraction (RHEED). The RHEED streaks, produced from the BTZ and BT layers, and their azimuthal positions showed perfect cube-on-cube epitaxial growth.

Standard θ-2θ x-ray diffraction (XRD) patterns were recorded using a Siemens D5000 diffractometer with Cu $K\alpha$ radiation. Figure 1 shows XRD patterns of seven BT/BTZ SL's and two films of parent compounds BT (thickness of about 2200 Å) and BTZ (thickness of about 4000 Å), grown on LSCO buffered MgO using the same targets and under similar deposition conditions as the SL's. These two single

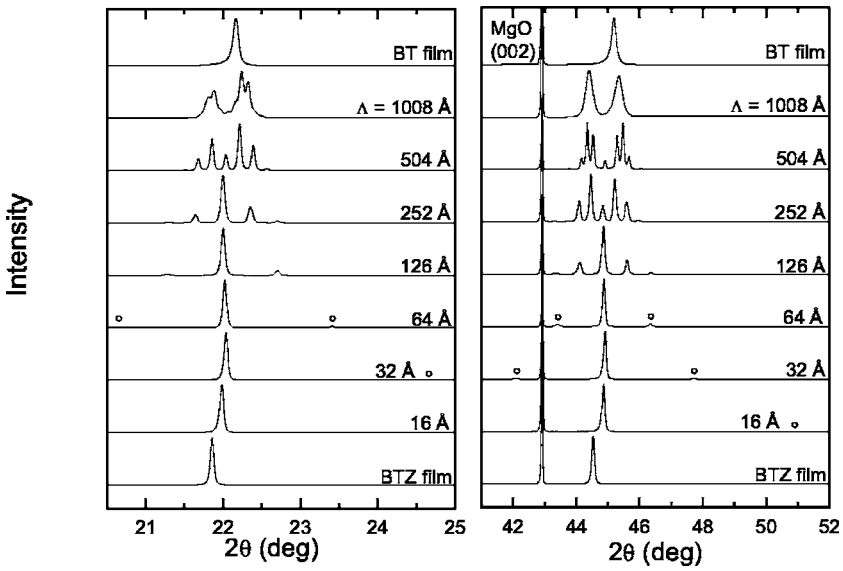

FIG. 1. θ-2θ x-ray diffraction for BT/BTZ SL's for $\Lambda = 16, 32, 64, 126, 252, 504, 1008$ Å, and for BT and BTZ films. For SL's with $\Lambda \leqslant 64$ Å, the circles (○) indicate the positions of the very weak intensity satellites peaks.

thin films were studied in order to compare them to our results on SL's. Figure 1 indicates that these BTZ and BT thin films are single-phase and well oriented since only one series of peaks is observed within the detection limits of our instrument. From the Bragg law we have determined the film out-of-plane lattice parameter of BTZ to be 4.067 Å, which is slightly larger than the bulk value. The value determined for BT is 4.011 Å, which is between the a_{BT}- and c_{BT}-bulk lattice parameters, and thus it is difficult to draw conclusions as to the growth direction and the tetragonality of the BT film.[22] For the SL's, we observe the so-called satellite peaks, typical of modulated structures, as well as their evolution as a function of Λ. The angular distance between the peaks determines Λ according to the Bragg formula $\sin \theta_n = n\lambda_x/2\Lambda$, where n is an integer and $\lambda_x = 1.5406$ Å is the radiation wavelength. We have performed model calculations following those reported in Refs. 13 and 23 in which we calculate the diffraction amplitude in a specular geometry using the interplanar spacings of the BT and BTZ as well as their individual thicknesses in each bilayer as adjustable parameters. Figure 2 illustrates the experimental diffractogram of the 504 Å SL along with the result of our model calculations. The high quality of fit is evident and the out-of-plane lattice parameter of BT (d_{BT}) and BTZ (d_{BTZ}) within the SL can be determined. The differences between experimental data and fitted curves can be attributed to the imperfect layer/layer interfaces which are not included in the model calculation.

Experimental XRD data for all SL's have been successfully fit and d_{BT} and d_{BTZ} were determined as a function of Λ. These values are presented in Fig. 3 along with the BT and BTZ bulk and single thin film values. For $\Lambda \geqslant 64$ Å, the out-of-plane value of the BT layers, $d_{BT} = 3.99$ Å, is approximately constant, is smaller than that of the BT film, and is very nearly that of the a_{BT} bulk value. This implies that the tensile stress in the BT superlattice layers is greater than that in the BT single film and suggests a structure in which the a axis of the BT layers in the BT/BTZ SL's is perpendicular to

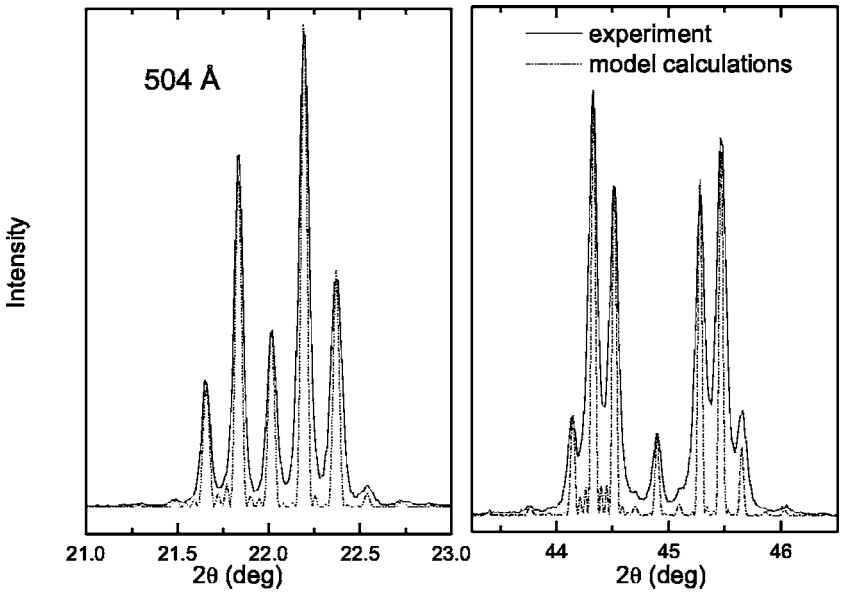

FIG. 2. The θ-2θ XRD pattern of the 504 Å SL and the result of the best model calculations (see text).

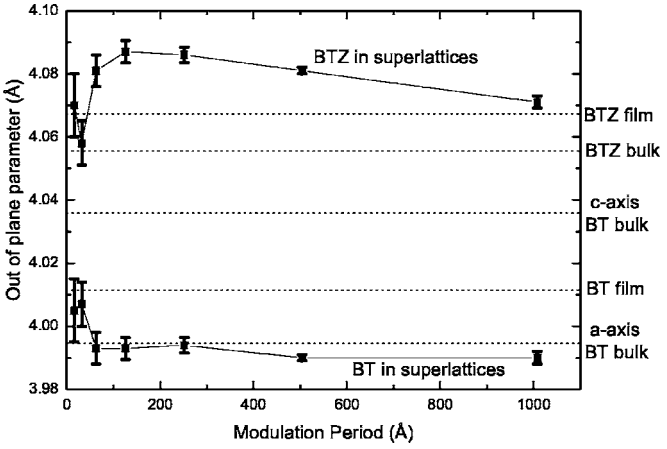

FIG. 3. Evolution of the out-of-lattice parameter of BT and BTZ layers in BT/BTZ SL's as a function of the modulation period Λ. The horizontal lines correspond to the lattice parameters of bulk BT and BTZ and to the out-of-plane lattice parameters of BT and BTZ single thin films.

the substrate. This is consistent with the fact that the *a*- or *c*-axis layer orientation is strongly dependent on the relative mismatch of the SL constituents. The lattice mismatch between the nominally cubic BTZ and the tetragonal BT *c* axis (0.47%) is smaller than that between the BT *a* axis (1.55%). Hence the BT *c* axis prefers to lie in the plane of the SL and the *a* axis is perpendicular to the plane. This is in contrast to BT/ST superlattices[2,3,12] where the *c* axis is observed to be normal to the plane. This is due to the smaller lattice mismatch between ST (a_{ST}=3.91 Å) and the BT *a* axis (−2.09% with a_{BT}) than with the BT *c* axis (−3.22% with c_{BT}). As to BTZ, we see in Fig. 3 that the out-of-plane parameter of BTZ single thin film is larger than the unit cell parameter of the bulk ceramic. This feature implies that the BTZ single film exhibits a tetragonal distortion due to the strain induced by the substrate. In the SL with the large modulation period (Λ=1008 Å) the d_{BTZ} value is very close to that in the BTZ film and it increases, in contrast to the BT layer behavior, as Λ decreases down to 126 Å. This implies that the BTZ layers are compressed in plane parallel to the substrate and exhibit enhanced tetragonal distortion which is induced by the mismatch between the alternating BTZ and BT layers. The increase of d_{BTZ} as Λ decreases suggests that strain is playing an increasingly important role compared to the partial stress relaxation produced by misfit dislocations. Finally, for the SL's with Λ=16 Å and 32 Å the d_{BT} value increases and approaches the out-of-plane parameter of the BT single film. Surprisingly, for SL's with Λ=16 and 32 Å the d_{BTZ} value decreases and also approaches the out-of-plane parameter of BTZ film. We will return to this point in our discussion of the Raman results.

The ferroelectric soft mode is usually very sensitive to the strain in thin films,[12,13,18,24] and so investigation of the soft mode behavior in ferroelectric SL's is very useful for better understanding of their physical properties. Raman spectroscopy is a suitable technique to detect the symmetry and type of domains (*c* or *a* domains) in single thin films and SL's since the Raman selection rules are strictly associated with the orientation of the polar axis. Raman measurements were performed using the 514.5 nm line from an argon ion laser and analyzed using a Jobin Yvon T64000 spectrometer equipped with a charge coupled device. An optical microscope was used to focus the incident light as a spot of about 1 μm in diameter on the sample. Polarized spectra were obtained in side-view backscattering geometry (for details see Ref. 24). Raman spectra have been measured on samples precisely oriented with respect to the crystallographic axes of BT layers: *Z* is perpendicular to the MgO substrate $Z\|[001]_{MgO}$, $Y\|[010]_{MgO}$, and $X\|[100]_{MgO}$. Vibrational spectra, and in particular the soft mode behavior, in BT single crystals have been extensively studied (see Ref. 25 and references therein). In the tetragonal ferroelectric BT (point group C_{4v} polar axis is along *Z*), the α_{zz} component of the Raman tensor involves A_1 phonons exclusively. For the α_{xx} and α_{yy} components the A_1 and B_1 phonons are allowed simultaneously, while *E* modes are only allowed for α_{zx} and α_{zy} components. In the tetragonal phase the *E*(1TO) soft mode is overdamped and according to the results reported by numerous authors and summarized by Scalabrin *et al.*[26] the soft mode frequency is about 34–38 cm^{-1}, while the halfwidth is about 85–115 cm^{-1}. In bulk BT crystals, the A_1(TO) component of the F_{1u} cubic soft mode at ~276 cm^{-1} is heavily damped and coupled with low-frequency A_1(TO) at 180 cm^{-1}. As a result of this coupling the sharp dip exists in $Y(ZZ)\bar{Y}$ spectrum while a sharp peak appears in the $Y(XX)\bar{Y}$ spectrum of the single-domain BT crystals.[26]

Figure 4 shows room-temperature Raman spectra recorded in $Y(ZX)\bar{Y}$, $Y(ZZ)\bar{Y}$, and $Y(XX)\bar{Y}$ scattering geometries for the BT/BTZ SL's and for the BT and BTZ single thin films. All spectra are corrected for the Bose-Einstein temperature factor. For the BT single thin film, the Raman spectra are very close to those of the bulk BT crystal[26] and confirm the tetragonal symmetry of this sample. *E* modes are observed in (*ZX*) spectrum and A_1 and B_1 modes in both (*XX*) and (*ZZ*) spectra. These latter spectra are very similar and the interference structure at 180 cm^{-1} is the same for both (*XX*) and (*ZZ*) spectra. This implies the absence of *c* domains, for which the polar axis is normal to the substrate, and the presence of 90° *a* and *b* domains in the BT thin single film. The *a* and *b* domains have their polar axes in the plane of substrate and are mutually perpendicular.

The polarization-dependent spectra of the BTZ single thin film confirm its epitaxial quality. Raman spectra presented in Fig. 4 are the first Raman results on an oriented BTZ compound, since polarized Raman data on single-crystalline BTZ have, to our knowledge, never been reported. As in bulk BTZ, the interference dip is shifted to lower wave numbers and appears at about 120 cm^{-1}. Absence of the overdamped soft mode in the low-frequency spectra of BTZ film is evident.

The Raman spectra of BT/BTZ SL's presented in Fig. 4 exhibit an obvious narrowing of the A_1(TO) and the *E*(TO) soft modes as compared to those of the BT single film. This result demonstrates that, contrary to the results that we reported on PMN/PT SL's,[18] the Raman spectra of BT/BTZ SL's do not reflect a simple superposition of the BT and BTZ

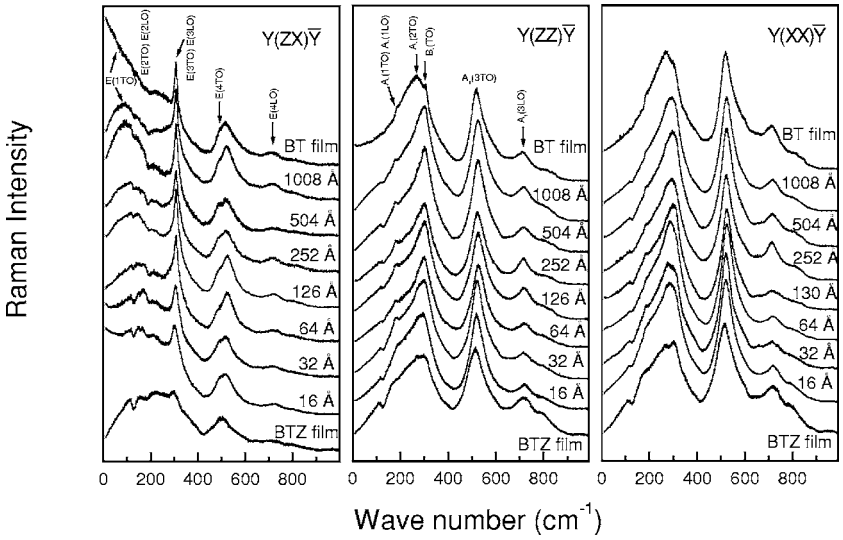

FIG. 4. Room-temperature Raman spectra for BT/BTZ SL's for $\Lambda = 16, 32, 64, 126, 252, 504, 1008$ Å, and for the BT and BTZ single thin films.

spectra, but give evidence of coupling between these constituent layers. The observed narrowing is a signature of the lattice ordering within the SL's. Scalabrin *et al.*[26] attributed the overdamped character of the Raman modes in BT crystal to the partial relaxation of the $q=0$ Raman selection rules due to the hopping of the Ti ions to equivalent off-center sites in the tetragonal phase. The question of the disorder of Ti in perovskites is still the subject of intensive investigation.[27–29] BTZ also exhibits a similar disorder and hence all Raman peaks are essentially broad.[20] This Ti disorder exists also in BT and BTZ single films, but in the SL's the strains imposed by the epitaxial superlattice construction seems to be significant in reducing the Ti disorder (we rule out the broadbands arising from films containing structural defects since these same structural defects would appear also in the superlattices since both films and superlattices were deposited under the same experimental conditions). The overall aspects of the polarized spectra for the $\Lambda \geqslant 64$ Å SL's, and especially the shape of the $A_1(1TO)$ mode at 180 cm^{-1} in the (XX) and (ZZ) geometries, establishes the tetragonal symmetry of the BT layers with the polar c axis parallel to the substrate. This also confirms the XRD results. As Λ decreases, we observe a broadening of some peaks [see for example $A_1(2TO)$ and $E(3TO)$] and the BTZ peaks begin to appear clearly in the SL spectra. In Fig. 4, the spectral profile for the $\Lambda \leqslant 32$ Å SL's is very close to that of the BTZ film. This suggests that the interlayer coupling between the BTZ and the BT layers increases and the effect of the Zr cations becomes increasingly important in the SL when the periodicity is small. This reinforces the idea that in the zero wavelength limit the BTZ/BT SL's for $\Lambda \leqslant 32$ Å can be considered as a mesoscopically modulated BTZ-BT solid solution, with the averaged concentration of Zr lower than $x=0.32$. This lower averaged concentration of the Zr cations could be produced either by a constant interface becoming progressively more important as the wavelength decreases, or by the Zr interdiffusion which could act to reduce the strain occuring in the small wavelength limit. This effect could also be responsible for the unexpected relaxation of the lattice parameters to the single thin film values exhibited in Fig. 3 for these short wavelength SL's.

The most significant feature of the SL's, with respect to the BT single crystal and the single thin film, are the upward frequency shifts of the $A_1(2TO)$ and the $E(1TO)$ soft modes. Being overdamped in BT single thin film the $E(TO)$ soft mode transforms to the underdamped peak in all SL's studied. The frequency of the $E(1TO)$ mode in the (XZ) spectra of all SL's and in the BT single film was determined using a fitting procedure. These results are presented in Fig. 5 (for 64 Å $\leqslant \Lambda \leqslant$ 1008 Å) together with the frequency reported for a bulk BT crystal.[26] We observe a significant upward shift of the $E(1TO)$ soft mode frequency when going from the BT single crystal to the BT single film. There is a second significant mode frequency shift in going from the BT single film to the SL's. In addition the frequency increases as Λ decreases.

Since for $\Lambda \leqslant 32$ Å the spectra reflect a large contribution from the BTZ layers, a determination of the BT layer $E(1TO)$ mode frequency is problematic. We attribute the upward shift of the soft modes and the narrowing of Raman peaks in SL's to the internal stress induced by the mismatch between BTZ and BT layers. The BTZ layers are compressed in the plane parallel to the film while the BT layers are under tensile stress. As follows from the observed soft mode hard-

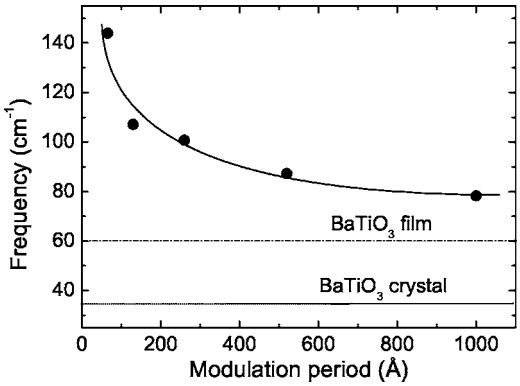

FIG. 5. The $E(1TO)$ soft mode frequency as a function of the modulation period Λ. The horizontal lines correspond to the frequency of $E(1TO)$ in the bulk BT single crystal and in the BT single thin film.

ening, the resulting modulated BTZ/BT lattice is much more rigid. It is worth noting that the soft mode stiffness is less pronounced $\Lambda > 252$ Å. This change at $\Lambda = 252$ Å can be attributed to partial stress relaxation at a critical layer thickness ($l_c = 126$ Å) above which it is energetically more favorable for dislocations to relax the strain in SL. We have observed the same effect in $BT_{\Lambda/2}/PT_{\Lambda/2}$ SL's at $l_c \sim 125$ Å (Ref. 13) and in the asymmetric $PMN_{(1-x)\Lambda}/PT_{x\Lambda}$ SL's at $l_c = 13$ Å of PT layer.[18] The similar values of l_c in BTZ/BT and BT/PT SL's is probably due to the close lattice mismatch of BT/BTZ and BT/PT SL's.

In summary, we have grown a series of lead-free ferroelectric/relaxor BT/BTZ SL's by PLD. Based on the excellent quality of x-ray patterns fits and on polarized Raman spectra, we conclude that the polar *c* axis of BT layers is parallel to the substrate due to the interlayer strains generated by the lattice mismatch between BTZ and BT. The Raman spectra of the SL's provide strong evidence that the BT and BTZ layers are coupled and that the narrowing of the Raman peaks, in contrast to the BT single thin film, suggests a reduction of the disorder of the Ti^{4+} ions due to the misfit strain. The strain is also responsible for the upward shift of the soft modes, especially the lowest $E(1TO)$ component, which is markedly altered with respect to its analogs in BT-bulk crystals and a BT single film. The soft-mode behavior as a function of wavelength indicates that the crystal structure in all SL's is more rigid than in BTZ and BT single films.

This work was supported by the Region of Picardy, the Regional European Development Funds, and RFBR (Grant No. 06-02-16271).

*Electronic address: mimoun.elmarssi@u-picardie.fr
†On leave from the Faculty of Physics, Rostov State University, Rostov-on-Don, Russia.

[1] H. Tabata, H. Tanaka, and T. Kawai, Appl. Phys. Lett. **65**, 1970 (1994).
[2] J. Kim, Y. Kim, Y. S. Kim, J. Lee, L. Kim, and D. Jung, Appl. Phys. Lett. **80**, 3581 (2002).
[3] L. Kim, D. Jung, J. Kim, Y. S. Kim, and J. Lee, Appl. Phys. Lett. **82**, 2118 (2003).
[4] T. Shimuta, O. Nakagawara, T. Makino, S. Arai, H. Tabata, and T. Kawai, J. Appl. Phys. **91**, 2290 (2002).
[5] K. Shimoyama, M. Kiyohara, K. Kubo, A. Uedono, and K. Yamabe, J. Appl. Phys. **92**, 4625 (2002).
[6] Can Wang, Q. F. Fang, Z. G. Zhu, A. Q. Jiang, S. Y. Wang, B. L. Cheng, and Z. H. Chen, Appl. Phys. Lett. **82**, 2880 (2003).
[7] H. N. Lee, H. M. Christen, M. F. Chishom, C. M. Rouleau, and D. H. Lowndes, Nature (London) **433**, 395 (2005).
[8] A. Q. Jiang, J. F. Scott, H. Lu, and Z. Chen, J. Appl. Phys. **93**, 1180 (2003).
[9] S. Rios, A. Ruediger, A. Q. Jiang, J. F. Scott, H. Lu, and Z. Chen, J. Phys.: Condens. Matter **15**, 305 (2003).
[10] Karen Johnston, Xiangyang Huang, J. B. Neaton, and Karin M. Rabe, Phys. Rev. B **71**, 100103(R) (2005).
[11] S. M. Nakhmanson, K. M. Rabe, and David Vanderbilt, Phys. Rev. B **73**, 060101(R) (2006).
[12] Rasmi R. Das, Yu. I. Yuzyuk, P. Bhattacharya, V. Gupta, and R. S. Katiyar, Phys. Rev. B **69**, 132302 (2004).
[13] F. Le Marrec, R. Farhi, M. El Marssi, J. L. Dellis, M. G. Karkut, and D. Ariosa, Phys. Rev. B **61**, R6447 (2000).
[14] S. E. Park and T. R. Shrout, J. Appl. Phys. **82**, 1804 (1997).
[15] H. Fu and R. E. Cohen, Nature (London) **403**, 281 (2000).
[16] V. Nagarajan, C. S. Ganpule, B. Nagaraj, S. Aggarwal, S. P. Alpay, A. L. Roytburd, E. D. Williams, and R. Ramesh, Appl. Phys. Lett. **75**, 4183 (1999).
[17] V. Nagarajan, S. P. Alpay, C. S. Ganpule, B. Nagaraj, S. Aggarwal, E. D. Williams, A. L. Roytburd, and R. Ramesh, Appl. Phys. Lett. **77**, 438 (2000).
[18] H. Bouyanfif, M. El Marssi, N. Lemée, F. Le Marrec, M. G. Karkut, and B. Dkhil, Phys. Rev. B **71**, 020103(R) (2005).
[19] J. Ravez and A. Simon, J. Korean Phys. Soc. **32**, S955 (1998).
[20] R. Farhi, M. El Marssi, A. Simon, and J. Ravez, Eur. Phys. J. B **9**, 559 (1999).
[21] J. Kreisel, P. Bouvier, M. Maglione, B. Dkhil, and A. Simon, Phys. Rev. B **69**, 092104 (2004).
[22] M. El Marssi, F. Le Marrec, I. A. Lukyanchuk, and M. G. Karkut, J. Appl. Phys. **94**, 3307 (2003).
[23] I. K. Schuller, Phys. Rev. Lett. **44**, 1597 (1980).
[24] Yu. I. Yuzyuk, R. S. Katiyar, V. A. Alyoshin, I. N. Zakharchenko, D. A. Markov, and E. V. Sviridov, Phys. Rev. B **68**, 104104 (2003).
[25] Yu. I. Yuzyuk, V. A. Alyoshin, I. N. Zakharchenko, E. V. Sviridov, A. Almeida, and M. R. Chaves, Phys. Rev. B **65**, 134107 (2002).
[26] A. Scalabrin, A. S. Chaves, D. S. Shim, and S. P. S. Porto, Phys. Status Solidi B **79**, 731 (1977).
[27] B. Zalar, V. V. Laguta, and R. Blinc, Phys. Rev. Lett. **90**, 037601 (2003).
[28] D. A. Tenne, A. Soukiassian, X. X. Xi, H. Choosuwan, R. Guo, and A. S. Bhalla, Phys. Rev. B **70**, 174302 (2004).
[29] B. Zalar, A. Lebar, J. Seliger, R. Blinc, V. V. Laguta, and M. Itoh, Phys. Rev. B **71**, 064107 (2005).